Rechargeable Lithium Batteries Hot Paper

International Edition: DOI: 10.1002/anie.201603897
German Edition: DOI: 10.1002/ange.201603897

# Organotrisulfide: A High Capacity Cathode Material for Rechargeable Lithium Batteries

*Min Wu, Yi Cui, Amruth Bhargav, Yaroslav Losovyj, Amanda Siegel, Mangilal Agarwal, Ying Ma, and Yongzhu Fu**

***Abstract:*** *An organotrisulfide (RSSSR, R is an organic group) has three sulfur atoms which could be involved in multi-electron reduction reactions; therefore it is a promising electrode material for batteries. Herein, we use dimethyl trisulfide (DMTS) as a model compound to study its redox reactions in rechargeable lithium batteries. With the aid of XRD, XPS, and GC-MS analysis, we confirm DMTS could undergo almost a $4e^-$ reduction process in a complete discharge to 1.0 V. The discharge products are primarily $LiSCH_3$ and $Li_2S$. The lithium cell with DMTS catholyte delivers an initial specific capacity of 720 $mAh\,g^{-1}{}_{DMTS}$ and retains 82 % of the capacity over 50 cycles at C/10 rate. When the electrolyte/DMTS ratio is 3:1 $mL\,g^{-1}$, the reversible specific energy for the cell including electrolyte can be 229 $Wh\,kg^{-1}$. This study shows organotrisulfide is a promising high-capacity cathode material for high-energy rechargeable lithium batteries.*

Rechargeable lithium batteries have attracted tremendous interest for portable electronics and electric vehicles owing to their high energy density.[1] Lithium-ion (Li-ion) batteries are based on the lithium intercalation chemistry of the anode and cathode materials, however, these have limited capacities and energy densities.[2] To increase their energy density, high-capacity electrodes need to be developed, such as sulfur cathode with a high theoretical specific capacity of 1672 $mAh\,g^{-1}$. However, the lithium–sulfur battery has several intrinsic difficulties that prevent it from practical applications.[3] Also attractive are organic electrode materials featuring high theoretical capacities, sustainability, and low cost.[3,4] Additionally, the unique traits of organic compounds, such as structural diversity and flexibility, make them promising electrode materials for rechargeable lithium batteries,[5] supercapacitors,[6] and redox flow batteries.[7] Organosulfide is a class of materials that could have favorable properties for battery application. In 1988, Visco and DeJonghe first investigated tetraethylthiuram disulfide as a cathode material for sodium batteries.[8] They found that the S–S bond can be reversibly broken and formed upon cycling, and a $2e^-$ redox reaction occurs. Whereafter, dimeric[9] and polymeric organodisulfides[5a,b,10] have been studied. However, organodisulfides have intrinsic drawbacks, such as slow kinetics and low capacities.[4]

To develop high-capacity cathode materials, we are exploring organotrisulfide (RSSSR, R is an organic group) for rechargeable lithium batteries. Organotrisulfide has a higher theoretical capacity than organodisulfide (RSSR). The extra middle sulfur atom in organotrisulfide can increase specific capacity and decrease the dissociation energy of the S–S bond. For example, the dissociation energy of the S–S bond in dimethyl disulfide (DMDS, $CH_3SSCH_3$) is about 70 $kcal\,mol^{-1}$,[11] whereas it is about 45 $kcal\,mol^{-1}$ in dimethyl trisulfide (DMTS, $CH_3SSSCH_3$).[12] The low dissociation energy could support fast electrode kinetics. Herein, we study DMTS as a model compound. DMTS has a theoretical capacity of 849 $mAh\,g^{-1}$ considering a $4e^-$ reduction reaction to form two lithium thiomethoxides ($LiSCH_3$) and one lithium sulfide ($Li_2S$), which is illustrated in Figure 1 a. Liquid DMTS is miscible with electrolyte to form a catholyte which can be evaluated in rechargeable lithium batteries. Inspired by our previous work on Li/polysulfide batteries,[13] binder-free multi-walled carbon nanotube (MWCNT) paper was used as the current collector and a reservoir for holding cycled products (Figure 1 b).

The open circuit voltage of the cell is about 2.4 V and the cell was discharged first to 1.7 V and cycled between 2.7–1.7 V at C/10 rate ($1C = 849\ mA\,g^{-1}$). The cutoff voltage of 1.7 V was used because $LiNO_3$ in the electrolyte is unstable at lower voltage.[14] $LiNO_3$ can passivate the lithium metal anode and reduce reactions between lithium metal and DMTS, therefore increasing cycling stability. The voltage profile shown in Figure 1 c demonstrates the Li/DMTS cell is rechargeable, and the first discharge curve consists of three voltage regions. The first discharge time is 8.5 h corresponding to 85 % of the theoretical discharge time (10 h) of DMTS. The charge process consists of a voltage plateau at about 2.2 V followed

[*] M. Wu, Y. Cui, A. Bhargav, M. Agarwal, Y. Fu
Department of Mechanical Engineering
Indiana University-Purdue University Indianapolis
Indianapolis, IN 46202 (USA)
E-mail: yongfu@iupui.edu
Y. Losovyj
Department of Chemistry, Indiana University
Bloomington, IN 47405 (USA)
A. Siegel, M. Agarwal, Y. Fu
Integrated Nanosystems Development Institute (INDI)
Indiana University-Purdue University Indianapolis
Indianapolis, IN 46202 (USA)
A. Siegel
Department of Chemistry and Chemical Biology
Indiana University-Purdue University Indianapolis
Indianapolis, IN 46202 (USA)
Y. Ma
Materials Science and Engineering Center
University of Wisconsin-Eau Claire
Eau Claire, WI 54702 (USA)

Supporting information for this article can be found under: http://dx.doi.org/10.1002/anie.201603897.

  

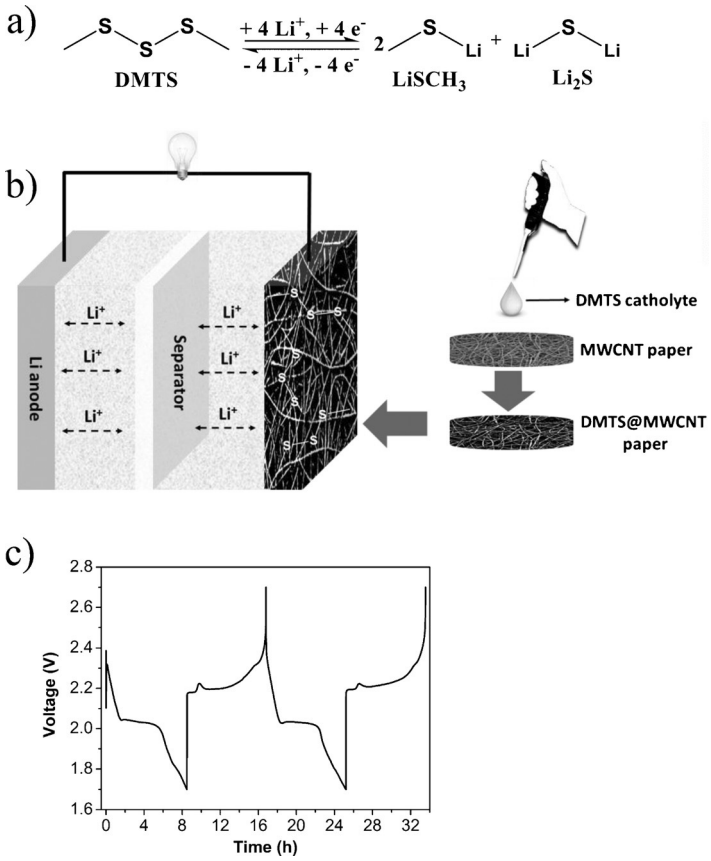


***Figure 1.*** a) The possible redox reaction of DMTS in a rechargeable lithium cell. b) Schematic illustration of the cell configuration and the addition of DMTS catholyte into a MWCNT-paper current collector. c) The voltage–time profile (initial two cycles) of the cell with $LiNO_3$-containing ether electrolyte cycled between 1.7–2.7 V at C/10 rate.

by gradual increase till the cutoff voltage. The second cycle shows the same voltage profile as the first one. The cyclic voltammogram (CV) profile of the cell shown in Figure S1 in Supporting Information reflects the voltage profile in Figure 1 c.

To reveal the reaction mechanism of DMTS, X-ray diffraction (XRD) was first conducted to identify the cycled products of DMTS. All samples were washed with DME completely to remove soluble species before the measurements. The discharged product of DMDS, which should be $LiSCH_3$ according to the disulfide/thiolate redox reaction mechanism,[9a] was used as a reference. The discharge voltage profile of DMDS is shown in Figure S2. As displayed in Figure 2 a, all the peaks arising from the discharge products of DMTS match very well with those of DMDS, indicating $LiSCH_3$ is a primary reduced product of DMTS. For the recharged electrode, only a strong peak at 26.0° is observed belonging to the (002) plane of MWCNTs,[15] meaning all the charged products were soluble species and washed away. The scanning electron microscopy (SEM) of the recharged electrode of DMTS only shows a clean MWCNT network with a negligible sulfur content, as shown in Figure S3.

X-ray photoelectron spectroscopy (XPS) was conducted to identify sulfur species in the discharged electrode of DMTS. Figure 2 b shows the XPS spectra of a discharged electrode at 1.7 V (sample I), discharged electrode at 1.0 V (sample II), and commercial $Li_2S$ sample (sample III) as a reference. The sample II was collected at low cutoff voltage to ensure complete reduction of DMTS; therefore $LiNO_3$ was not used in the electrolyte. The commercial $Li_2S$ shows standard S $2p_{3/2}$ and S $2p_{1/2}$ doublet peaks centered at 160.1 and 161.3 eV (see Figure S4 and Tables S1–3 for binding energy calibration and fitting details), respectively.[16] The S $2p_{3/2}$ peak centered at 161.6 eV is attributed to the impurity in the sample. The sample I shows three S $2p_{3/2}$ peaks at 163.2, 161.6, and 160.1 eV. The S $2p_{3/2}$ peak centers at 160.1 eV is attributed to $Li_2S$, confirming $Li_2S$ is another discharged product of DMTS.[16] Although no main peaks of $Li_2S$ are seen in the XRD pattern in Figure 2 a, it can be concluded here that the formed $Li_2S$ is in an amorphous state.[13] According to the recent literature,[17] the S $2p_{3/2}$ peaks located at 161.6 and 163.2 eV can be attributed to $LiSCH_3$ and $LiSSCH_3$ (the S bonded with the $CH_3$ group), respectively. The XPS spectrum for the sample II displays two main S $2p_{3/2}$ peaks centered at 160.1 and 161.6 eV, which are ascribed to $Li_2S$ and $LiSCH_3$, respectively. The sulfur peak area ratio in $LiSCH_3$ and $Li_2S$ is far less than 2:1, which could be due to the loss of $LiSCH_3$ in the washing process. Compared to sample I, the sulfur doublets for $LiSCH_3$ and $Li_2S$ in the sample II increase while the sulfur doublet for $LiSSCH_3$ decreases, indicating a further conversion of $LiSSCH_3$ to $LiSCH_3$ and $Li_2S$. This comparison also indicates that $LiSSCH_3$ is an incomplete discharged product of DMTS if the cutoff voltage is 1.7 V and the discharged products are almost completely $Li_2S$ and $LiSCH_3$ if the cutoff voltage is 1.0 V. The discharge capacity obtained for the sample II is

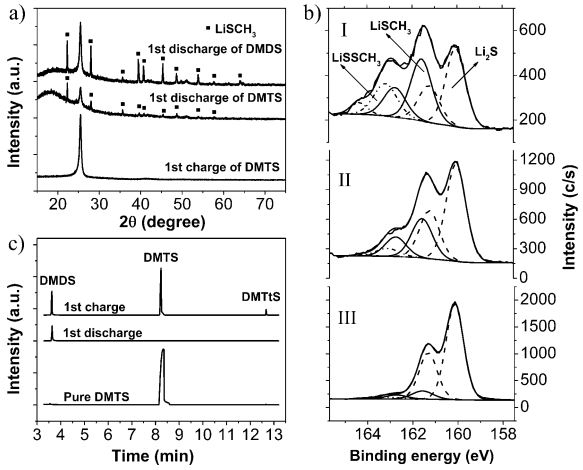


***Figure 2.*** a) XRD patterns of the discharged electrode of DMDS, the discharged and recharged electrode of DMTS. b) XPS analysis of the discharged sample of DMTS at 1.7 V (I), discharged sample of DMTS at 1.0 V (II), and the commercial $Li_2S$ (III). c) GC-MS spectra of pure DMTS, the vapor samples from the discharged electrode I (1st discharge) and recharged electrode (1st charge) of DMTS.

  

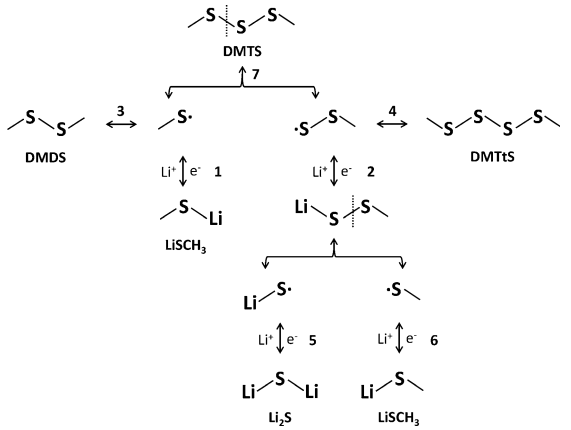


***Scheme 1.*** Redox reactions of dimethyl trisulfide (DMTS) in rechargeable lithium batteries. See text for details.

819 mAh g$^{-1}$ (Figure S5), corresponding to 96% of the theoretical capacity of DMTS. In other words, each DMTS can take up to 3.8 e$^-$ in a complete discharge.

To identify the charged products of DMTS, we turned to gas chromatography–mass spectrometry (GC-MS). A carbon fiber microextraction probe was used to collect the vapor of these samples to avoid the salt contamination on the instrument. Pure DMTS shows a strong peak at the retention time of 8.4 min in GC in Figure 2c and the highest mass/charge ratio ($m/z$ 126) shown in MS in Figure S6 can be attributed to DMTS. The discharged sample collected at 1.7 V shows no peak at 8.4 min, but instead a small peak at 3.6 min. The $m/z$ 94 signal shown in Figure S6 confirms the discharged sample is DMDS. The recharged sample shows three peaks at 3.6, 8.4, and 12.6 min corresponding to DMDS, DMTS, and dimethyl tetrasulfide (DMTtS), respectively, which are identified based on the $m/z$ ratios in Figure S6. Two negligible peaks at 3.6 and 12.6 min are also seen in the DMTS sample, meaning the recharged electrode contains small amounts of DMDS and DMTtS.

From the analysis of XRD, XPS, and GC-MS, we can formulate the redox reactions of DMTS. In the incomplete discharge process with a high cutoff voltage, that is, 1.7 V, $LiSCH_3$ and $Li_2S$ are the primary discharge products, and $LiSSCH_3$ and DMDS are the minor ones. The primary recharged product is the starting material, that is, DMTS. Some DMDS and DMTtS co-exist in the recharged products. The redox reactions of DMTS in rechargeable lithium batteries are elaborated in Scheme 1. First, the S–S bond in DMTS could undergo homolytic cleavage into two radicals $^{\bullet}SCH_3$ and $^{\bullet}SSCH_3$ due to favorable kinetics and stabilization of the $^{\bullet}SSCH_3$ radical through the 3 e$^-$ $\pi$ bond.[18] These radicals react with $Li^+$ and e$^-$ to form thiolates (reactions 1 and 2 in Scheme 1), i.e., $LiSCH_3$ and $LiSSCH_3$, or combine to form shorter-chain DMDS (reaction 3) or longer-chain DMTtS (reaction 4). Because the geometry of the HOMO (3p orbital) of the sulfur in $^{\bullet}SCH_3$ and $^{\bullet}SSCH_3$ is symmetric with that of the LUMO (2s orbital) in $Li^+$, and their orbital potential energies are close to each other ($\Delta E <$ 12 eV), radicals $^{\bullet}SCH_3$ and $^{\bullet}SSCH_3$ tend to react with $Li^+$ and e$^-$ to form $LiSCH_3$ and $LiSSCH_3$, respectively, as expressed in Figure S7.[19] A large number of mobile Li ions ensure primarily the lithiated reactions 1 and 2, even though the self-formation of DMDS and DMTtS from radicals cannot be excluded. The formed DMTtS would soon get reduced and cannot be detected by GC-MS because the dissociation energy of the S–S bond in DMTtS is even lower than that in DMTS.[11] The formed DMDS is reduced to $LiSCH_3$ at a voltage of 1.9 V.[17] $LiSSCH_3$ continues to be reduced through the S–S bond breaking in reaction 5 and 6 because of the excess of Li ions. In the recharge step, $Li_2S$ and all these thiolates are de-lithiated, which result in the small peak at 2.2 V in the voltage profile (Figure 1c) due to activation barriers. The radicals $^{\bullet}SCH_3$ and $^{\bullet}SSCH_3$ are formed and they can be combined into DMDS, DMTS (reaction 7), and DMTtS which were detected in GC-MS. We believe other longer sulfides or elemental sulfur are unlikely to be formed.

The battery performance of DMTS with mass loading of 6.7 mg cm$^{-2}$ was measured. The electrolyte/DMTS ratio in the cell is 5.7:1 mL g$^{-1}$. Figure 3a presents the cycling performance and Coulombic efficiency of the cell at C/10 rate. The initial discharge capacity is up to 720 mAh g$^{-1}$. After 50 cycles, the discharge capacity is 590 mAh g$^{-1}$, retaining 82% of the initial capacity. The Coulombic efficiency is up to 98% for most cycles. The corresponding voltage–capacity profiles are displayed in Figure S8. The SEM image and elemental mappings in Figure S9 show the nanopores in the MWCNTs network are filled with the discharged products. The cycled lithium anode is passivated by sulfur-containing species, as shown in Figure S10, indicating the shuttle effect also occurs in the Li/DMTS cell as in Li–S batteries,[13] which results in cycling degradation.

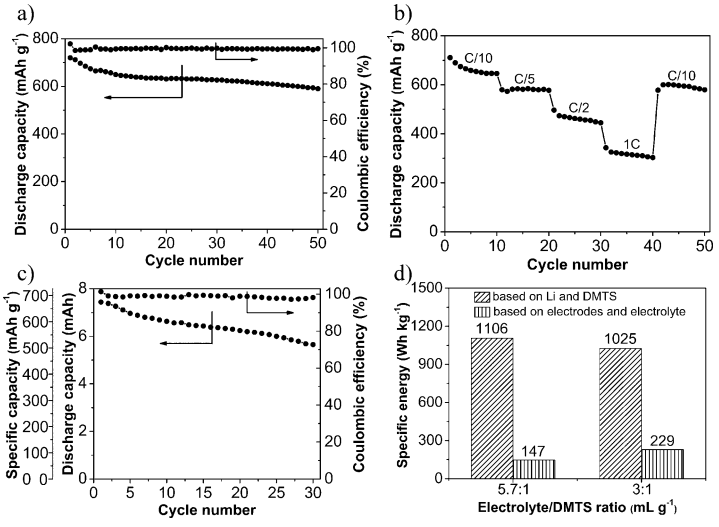


***Figure 3.*** a) The cycling performance and Coulombic efficiency of a cell cycled between 1.7–2.7 V at C/10 rate with DMTS loading of 6.7 mg cm$^{-2}$. b) Rate performance of a cell with DMTS catholyte. c) The cycling performance and Coulombic efficiency of a cell cycled between 1.7–2.7 V at C/10 rate with DMTS loading of 11.3 mg cm$^{-2}$. d) The specific energies of two cells with different electrolyte/DMTS ratios after five cycles, the specific energy is calculated based on either the mass of lithium and DMTS or the mass of electrodes and electrolyte.

  

The rate performance of a cell with the DMTS catholyte is shown in Figure 3b. The cell shows discharge capacities of 658, 582, 462, and 317 mAh $g^{-1}$ at C/10, C/5, C/2, and 1C, respectively. At each rate, the discharge capacity slowly decreases with cycles. When the rate returned to C/10, the discharge capacity recovered to 597 mAh $g^{-1}$. After 50 cycles, the discharge capacity is 580 mAh $g^{-1}$, which retains 81 % of the initial capacity at C/10 rate. The corresponding representative voltage profiles at different rates are shown in Figure S11.

To demonstrate a high energy density battery, we further reduced the electrolyte/DMTS ratio in the cell to 3:1 mL $g^{-1}$. Figure 3c shows the cycling performance of the cell with high DMTS loading of 11.3 mg $cm^{-2}$ at C/10 rate. The initial discharge capacity is up to 7.42 mAh, corresponding to a specific discharge capacity of 675 mAh $g^{-1}$. After 30 cycles, the cell discharge capacity is still as high as 5.67 mAh. The Coulombic efficiency is above 98 % for all cycles. For comparison, we made a Li/polysulfide cell with the same MWCNT paper, the sulfur loading is 7.4 mg $cm^{-2}$ and the electrolyte/sulfur ratio is 6.9:1 mL $g^{-1}$. The cell shows an initial discharge capacity of 6.70 mAh at C/10 rate as shown in Figure S12, but cannot be cycled anymore after 24 cycles. The discharge capacity decreases to 4.11 mAh and the Coulombic efficiency decreases to 64.4 %. The optimal electrolyte/sulfur ratio in Li-S batteries is typically $\geq$10 mL $g^{-1}$, which is too high to achieve a high specific energy.[20] Based on the theoretical capacities of electrodes (DMTS and lithium) and average cell voltage of approximately 2.0 V, the Li/DMTS battery has a high specific energy of 1391 Wh $kg^{-1}$, which is higher than those of Li-ion batteries and other rechargeable lithium batteries, as shown in Figure S13. The specific energies in the 5th cycle in terms of the electrodes and cell (electrodes and electrolyte) with the electrolyte/DMTS ratio of 3:1 mL $g^{-1}$ are 1025 Wh $kg^{-1}$ and 229 Wh $kg^{-1}$, respectively, as shown in Figure 3d. The specific energy for the cell is even higher than those of most reported Li–S batteries due to the low electrolyte/DMTS ratio.[13,20,21] When the electrolyte/DMTS ratio is further reduced to 2:1 mL $g^{-1}$, the specific energy of the cell in the 5th cycle increases to 244 Wh $kg^{-1}$, but the cell performance degrades rapidly (Figure S14). The theoretical energy density of DMTS is 2021 Wh $L^{-1}$, which is also higher than those of other cathode materials (Figure S13).

In summary, we have demonstrated that dimethyl trisulfide is a potential cathode material for rechargeable lithium batteries. The XRD and XPS analysis on the first discharged electrodes indicates the discharge is almost a 4 $e^-$ reduction process and the discharge products are mostly $LiSCH_3$ and $Li_2S$. The GC-MS results confirm the recharged products consist of DMTS (major product), DMDS, and DMTtS. Using an ether-based electrolyte with $LiNO_3$ additive, DMTS can sustain prolonged cycles in a binder-free MWCNT current collector. The cell delivers an initial capacity of 720 mAh $g^{-1}_{DMTS}$ and retains 82 % of the initial capacity over 50 cycles with DMTS loading of 6.7 mg $cm^{-2}$ at C/10 rate. When the electrolyte/DMTS ratio is decreased to 3:1 mL $g^{-1}$, the specific energy for the cell including electrolyte is 229 Wh $kg^{-1}$. This study reveals the redox reaction mechanism of DMTS, thereby shedding light on the development of high capacity organotrisulfide-based cathode materials for rechargeable lithium batteries.

## Acknowledgements

This work was supported by the startup grant from Purdue School of Engineering and Technology at Indiana University-Purdue University Indianapolis. We acknowledge the Integrated Nanosystems Development Institute for use of their XRD and SEM, which were awarded through the NSF grants MRI-1429241 and MRI-1229514, respectively. We thank the Nanoscale Characterization Facility at Indiana University for XPS use.

**Keywords:** cathode materials · dimethyl trisulfide · organotrisulfides · rechargeable lithium batteries · redox reactions

**How to cite:** *Angew. Chem. Int. Ed.* **2016**, *55*, 10027–10031
*Angew. Chem.* **2016**, *128*, 10181–10185

[1] M. Armand, J.-M. Tarascon, *Nature* **2008**, *451*, 652–657.
[2] J. B. Goodenough, Y. Kim, *Chem. Mater.* **2010**, *22*, 587–603.
[3] Y. Liang, Z. Tao, J. Chen, *Adv. Energy Mater.* **2012**, *2*, 742–769.
[4] Z. Song, H. Zhou, *Energy Environ. Sci.* **2013**, *6*, 2280–2301.
[5] a) N. Oyama, T. Tatsuma, T. Sato, T. Sotomura, *Nature* **1995**, *373*, 598–600; b) Z. Song, H. Zhan, Y. Zhou, *Chem. Commun.* **2009**, 448–450; c) K. Zhang, C. Guo, Q. Zhao, Z. Niu, J. Chen, *Adv. Sci.* **2015**, *2*, 1500018; d) Z. Song, Y. Qian, M. L. Gordin, D. Tang, T. Xu, M. Otani, H. Zhan, H. Zhou, D. Wang, *Angew. Chem. Int. Ed.* **2015**, *54*, 13947–13951; *Angew. Chem.* **2015**, *127*, 14153–14157.
[6] G. A. Snook, P. Kao, A. S. Best, *J. Power Sources* **2011**, *196*, 1–12.
[7] F. R. Brushett, J. T. Vaughey, A. N. Jansen, *Adv. Energy Mater.* **2012**, *2*, 1390–1396.
[8] S. J. Visco, L. C. DeJonghe, *J. Electrochem. Soc.* **1988**, *135*, 2905–2909.
[9] a) M. Liu, S. J. Visco, L. C. De Jonghe, *J. Electrochem. Soc.* **1989**, *136*, 2570–2575; b) S. J. Visco, M. Liu, L. C. DeJonghe, *J. Electrochem. Soc.* **1990**, *137*, 1191–1192.
[10] a) K. Naoi, K. I. Kawase, M. Mori, M. Komiyama, *J. Electrochem. Soc.* **1997**, *144*, L173–L175; b) N. Oyama, *Macromol. Symp.* **2000**, *159*, 221–227; c) S.-R. Deng, L.-B. Kong, G.-Q. Hu, T. Wu, D. Li, Y.-H. Zhou, Z.-Y. Li, *Electrochim. Acta* **2006**, *51*, 2589–2593.
[11] T. L. Pickering, K. Saunders, A. V. Tobolsky, *J. Am. Chem. Soc.* **1967**, *89*, 2364–2367.
[12] E. L. Clennan, K. L. Stensaas, *Org. Prep. Proced. Int.* **1998**, *30*, 551–600.
[13] Y. Fu, Y. S. Su, A. Manthiram, *Angew. Chem. Int. Ed.* **2013**, *52*, 6930–6935; *Angew. Chem.* **2013**, *125*, 7068–7073.
[14] S. S. Zhang, *J. Electrochem. Soc.* **2012**, *159*, A920–A923.
[15] M. Wu, Y. Cui, Y. Fu, *ACS Appl. Mater. Interfaces* **2015**, *7*, 21479–21486.
[16] Z. Li, S. Zhang, C. Zhang, K. Ueno, T. Yasuda, R. Tatara, K. Dokko, M. Watanabe, *Nanoscale* **2015**, *7*, 14385–14392.
[17] S. Chen, F. Dai, M. L. Gordin, Z. Yu, Y. Gao, J. Song, D. Wang, *Angew. Chem. Int. Ed.* **2016**, *55*, 4231–4235; *Angew. Chem.* **2016**, *128*, 4303–4307.
[18] R. Steudel, *Chem. Rev.* **2002**, *102*, 3905–3946.
[19] G. L. Miessler, P. J. Fischer, D. A. Tarr, *Inorganic Chemistry*, *5th ed.*, Pearson Education: Upper Saddle River, N. J. 2013, pp. 134–136.

  

[20] a) S. Zhang, *Energies* **2012**, *5*, 5190 – 5197; b) M. Hagen, D. Hanselmann, K. Ahlbrecht, R. Maça, D. Gerber, J. Tübke, *Adv. Energy Mater.* **2015**, *5*, 1401986.

[21] C. Zu, A. Manthiram, *Adv. Energy Mater.* **2014**, *4*, 1400897.

Received: April 21, 2016
Published online: July 13, 2016

  